NUMERICAL STUDY OF TURBULENT LEAN PREMIXED METHANE-AIR FLAMES

B. YILMAZ
Marmara University
byilmaz@eng.marmara.edu.tr

S. ÖZDOĞAN
Marmara University
sozdogan@eng.marmara.edu.tr

I. GÖKALP
Icare-cnrs
gokalp@cnrs-orleans.fr

Abstract

Lean Premixed Combustion (LPC) is recently proposed in gas turbine combustors which have been operated traditionally in the non-premixed mode. In this method, fuel and air are mixed before entering the combustor. With LPC, the flame temperature is reduced due to the operating with excess air conditions. Thus, thermal NO_x can be reduced to negligible levels at these lean conditions. On the other hand, the local and global flame extinction risks and therefore flame instabilities may arise because of operating at fuel-lean conditions near the lean flammability limit. In order to control such flames, both their chemical kinetics and flame propagation properties should be investigated in detail, mainly for various equivalence ratios.

In this study, the numerical simulations based on experimental data obtained from the combustion chamber setup of the ICARE are performed. The experimental results concern turbulent premixed methane-air flames stabilized on a Bunsen type burner; they are obtained by LDA for the cold and hot flow velocity statistics and by laser induced Mie and Rayleigh scattering techniques for flame front statistics. The operating conditions in experiments are chosen to be close to the gas turbine combustor operating conditions. Numerical simulations are performed by using the Fluent® software. Both the analysis of the flow and turbulence properties of the chamber by using the k-Ů turbulence model and its variants and the premixed flame properties of the methane/air mixtures are investigated. The influence of the equivalence ratio on the flame properties is examined as well. It is observed that increase in equivalence ratio results in decrease in the flame length and the flame brush thickness. Similar tendencies are observed in the experiments. Flame front properties are examined with the combustion model provided by the Fluent® software, namely Zimont premixed model, and y the well-known CFM turbulent premixed combustion model. Satisfactory results are obtained.

Keywords: *Turbulent combustion, premixed, methane-air, CFM*

1. Introduction

Gas turbine combustors have generally been operated in the non-premixed mode for safety and stability reasons. In order to achieve low level NOx emissions, besides other methods Lean Premixed Combustion (LPC) is recently proposed. In this method, fuel and air are mixed before entering the combustor. With LPC, the flame temperature is reduced due to the operation with excess air conditions. Thus, thermal NOx can be reduced to negligible levels at these lean conditions. On the other hand, the local and global flame extinction risks and therefore flame instabilities may arise because of operating at fuel-lean conditions near the lean flammability limit. In order to control such flames, both their chemical kinetics and flame propagation properties should be investigated in detail, mainly for various equivalence ratios.

In this study, the numerical simulations based on experimental data obtained from the combustion chamber setup of the ICARE [1,2] are performed. The experimental results concern turbulent premixed methane-air flames stabilized on a Bunsen type burner; they are obtained by LDA for the cold and hot flow velocity statistics and by laser induced Mie and Rayleigh scattering techniques for flame front statistics. The operating conditions in experiments are chosen to be close to the gas turbine combustor operating conditions by applying constant average burner exit velocity [2].

The flow field in the combustion chamber is developed by the interaction of both turbulence and combustion. Therefore, the numerical simulations are performed in two stages using the Fluent software. The analysis of the turbulent flow field inside the chamber space without reaction is initially examined. The standard ***kï Ů*** turbulence model and its variants are applied along with the modifications proposed in several works [3-6]. In the second stage, the premixed flame statistics of the methane/air mixtures are investigated by means of two different turbulent premixed combustion models.

Zimont turbulent premixed combustion model described in [7,8,15] provided by Fluent is investigated first. This model is based on the solution of the progress variable transport equation and is strictly applicable when the smallest turbulent eddies in the flow are smaller than the flame thickness, and penetrate into the flame zone.

The effect of the equivalence ratio on the flame properties is also examined with Zimont model. The physical properties of the mixture at different operating conditions are obtained from CHEMKIN II software package[16].

It is found that with increasing equivalence ratio both the flame tip length and the flame brush thickness decrease. Similar tendencies are observed in the experiments.

The CFM model is also examined in this study. This well-known flame surface density model is added to the Fluent by means of user defined functions utilities. Both the analysis of the flame properties and the prediction of the consumption/production rates of species become possible with this model. The flame front results including flame surface density distribution are compared to both experiments and those of Zimont model.

2. Experimental setup

The experimental setup is a stainless steel cylindrical combustion chamber operated up to 1 MPa with inner diameter of 300 mm[1,2]. The chamber consists of two 600 mm water-cooled vertical cylinders on each there are 4 windows for accessing optical diagnostics Figure1.

The burner is an axisymmetric Bunsen type burner placed at the bottom of the chamber. It can be moved vertically through the chamber space. The inner diameter is 25 mm. A perforated plate is located 50 mm upstream of the burner exit in order to generate turbulence. Stoichiometric methane-air pilot flame is used to stabilize the lean premixed flame.

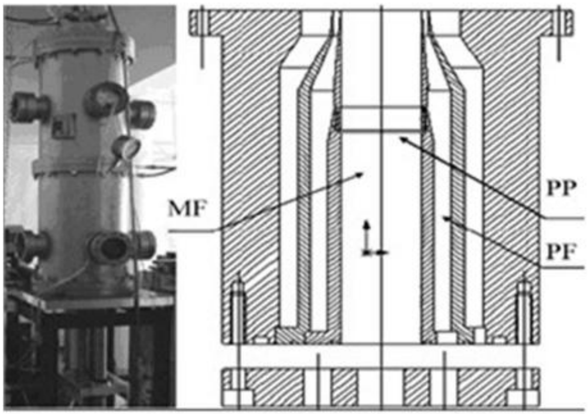

Figure 1. Combustion chamber setup and schematic view of the burner. (PF, pilot flame flow channel; PP, perforated plate; and MF, main premixed flow section.)

Air is assumed to be working fluid flow in cold flow turbulence measurements which are performed by using LDA techniques.

For reactive case measurements, Mie and Rayleigh scattering diagnostics are used to obtain flame front properties.

3. Governing Equations

The turbulent flow field is described by Favre-averaged Navier-Stokes equations in conservative form. Besides the continuity and momentum equations two more equations are solved which are defined by the well known $k-\varepsilon$ turbulence model in the following form,

$$\frac{\partial \rho k}{\partial t} + \frac{\partial}{\partial x_i}(\rho k u_i) = \frac{\partial}{\partial x_i}\left((\mu + \frac{\mu_t}{\sigma_k}) \frac{\partial k}{\partial x_i} \right) + G_k - \rho\varepsilon \quad (1)$$

$$\frac{\partial \rho \varepsilon}{\partial t} + \frac{\partial}{\partial x_i}(\rho \varepsilon u_i) = \frac{\partial}{\partial x_i}\left((\mu + \frac{\mu_t}{\sigma_\varepsilon}) \frac{\partial \varepsilon}{\partial x_i} \right) + C_{\varepsilon 1}\frac{\varepsilon}{k} G_k - C_{\varepsilon 2}\rho\frac{\varepsilon^2}{k} \quad (2)$$

Turbulent viscosity is defined as,

$$\mu_t = \rho C_\mu \frac{k^2}{\varepsilon} \quad (3)$$

In these equations, G_k represent the generation due to the mean velocity. The constants of these models are,

$C_{\varepsilon 1}$=1.44, $C_{\varepsilon 2}$=1.92, C_{ε}=0.09, σ_k=1.0, σ_ε=1.3.

In many premixed combustion devices, combustion takes place in a thin flame sheet which separates unburnt premixed reactants and burnt products. The Zimont model considers that the reaction takes place in this region and flame front moves toward unburnt species. In this approach, the flame front propagation is modeled by solving a transport equation for Favre averaged reaction progress variable: *c*, denoted by:

$$\frac{\partial \rho c}{\partial t}+\frac{\partial}{\partial x_i}(\rho u c)=\frac{\partial}{\partial x_i}\left(\frac{\mu_t}{Sc_t}\frac{\partial c}{\partial x_i}\right)+\rho S_c \qquad (4)$$

In this equation, Sc_t and S_c are turbulent Schmidt number and the reaction progress source term, respectively.

The progress variable is defined as a normalized sum of the product species as in the following equation. It takes the value of 0 and 1 in the fresh and the product gases regions of the flow, respectively.

$$c=\sum_{i=1}^{n} Y_i \Big/ \sum_{i=1}^{n} Y_{i,eq} \qquad (5)$$

An algebraic closure for the source term in Equation 4 is proposed by Zimont et al [7] to be,

$$\rho S_c=\rho_u U_t |\nabla c| \qquad (6)$$

and turbulent flame speed U_t is defined as,

$$U_t = A(u')^{3/4} U_l^{1/2} \alpha^{-1/4} l_t^{1/4} \qquad (7)$$

where *A* is the model constant proposed to be 0.52 for methane air mixtures [7]. U_l is the laminar flame speed, α is the thermal diffusivity of the unburnt mixture. In order to take stretch effect into account, the source term for the progress variable is multiplied by a factor which controls the quenching probability of the flame [15].

An alternative model for the turbulent premixed combustion is the flame surface density approach, summarized in [10]. In this model, an extra scalar transport equation given in the following form is solved.

$$\frac{\partial \Sigma}{\partial t}+\frac{\partial}{\partial x_i}(\rho u \Sigma)=\frac{\partial}{\partial x_i}\left(\frac{\nu_t}{\sigma_c}\frac{\partial \Sigma}{\partial x_i}\right)+\kappa_m \Sigma+\kappa_t \Sigma - D \qquad (8)$$

The first term on the right hand side of the equation represents the diffusion of the flame surface due to turbulent flow. The second and third terms indicate the production of the flame surface by turbulence due to mean flow gradients and local turbulence conditions. The last term represents the destruction. There are several approaches to model production and destruction source terms [10-12].

In present study, the well - known CFM model is examined. The source terms are described as in Table 1 by this model.

κ_m	κ_t	D
$A_{ik}\dfrac{\partial u_k}{\partial x_i}$	$\alpha_o \dfrac{\varepsilon}{k}$	$\beta_o \dfrac{S_L + C\sqrt{k}}{Y/Y_u}\Sigma^2$

Table 1. The modeled source terms in Equation 8.

The κ_m term is often neglected comparing to the κ_t term [10,13]. The model constants, α_0, β_o and *C*, are defined as 1.7, 1.0 and 0.5, respectively, in [11,12].

A modification for the pre-constant of κ_t term is proposed in [13]. They investigate the average flame position numerically and compare the turbulent flame speed parameter with measured data. It is reported that the tuning of this term leads to relatively well predicted flame shapes comparing to the experiments. They also observe that the CFM model with original constants underestimates the reaction rate. This modified version of the CFM model, abbreviated as the MCFM model in this text, is also tested.

Species equations for one step methane-air reaction are also solved besides the flame surface transport equation. The source terms of the species equations are closed by the computed flame surface density. This closure is defined as,

$$\dot{w}_F = -\rho_o I_o S_L Y_o \Sigma \qquad (9)$$

where ρ_o and Y_o, represent the unburnt fuel density mass fraction, respectively. S_L is the laminar flame speed. I_o represents the stretch factor equal to 1.

Grid generated turbulence conditions are introduced by turbulent kinetic energy and dissipation rate profiles extracted from measured data.

Physical properties of the mixtures at different equivalent ratio conditions necessary for the reactive case studies are obtained by PREMIX code of the CHEMKIN II package [16]. The laminar flame speeds and adiabatic flame temperatures are also generated by using this package.

All the simulations are performed at atmospheric pressure conditions. 300 K is introduced as an initial mixture temperature.

4. Results and Discussion

The cold flow simulations are performed initially in order to resolve the turbulent characteristics of the flow. Air is assumed to be working fluid as used in experiments.

An axisymmetric and two-dimensional model is developed for the geometry. Then, the chamber space is meshed with structured fine meshes near the burner exit and as well as the mixing effective regions. The gradients of the flow and the premixed flame parameters are expected to be relatively high in these regions. On the other hand, the coarse meshes are used for the regions far from the burner exit due to the computational cost and time.

The conical jet flow becomes turbulent mainly by the perforated plate used in burner section and the shear interaction of the main flow and the surrounding air inside the combustion chamber. This turbulence field is modeled by well known k-ε turbulence model. Several variants of k-ε model provided by Fluent library, such as RNG and realizable k-ε models are also examined. Moreover, in order to resolve round jet-plane jet anomaly, modifications proposed for this model in several articles are examined. Morgans et al [4] proposes to modify $C_{\varepsilon 1}$ to 1.6 instead of 1.44. The modification for $C_{\varepsilon 2}$ to be 1.92 is proposed in [3]. Pope correction [5,6] is also imposed by adding a user defined function to Fluent.

Comparison of the mean velocity distributions in normalized axial direction shows that modified versions of k-ε turbulence model results are in better agreement with experiments than the standard one as shown in Figure 2. The $C_{\varepsilon 1}$ modification gives the most satisfactory result for mean velocity profile. The turbulence core decay is estimated about three diameters after the burner exit in both simulations and experiments.

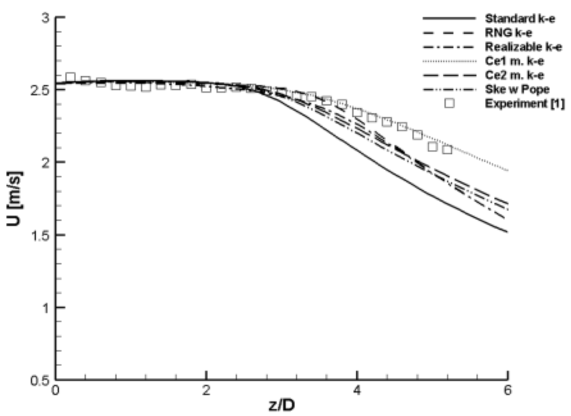

Figure 2. **Mean velocity distributions along normalized symmetry axis. (Inner chamber diameter, D, is 25 mm)**

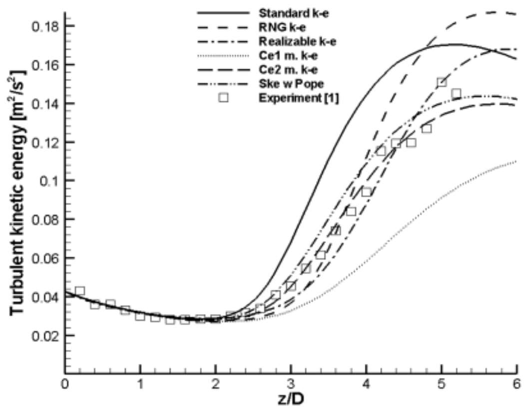

Figure 3. Turbulent kinetic energy distributions along normalized symmetry axis.

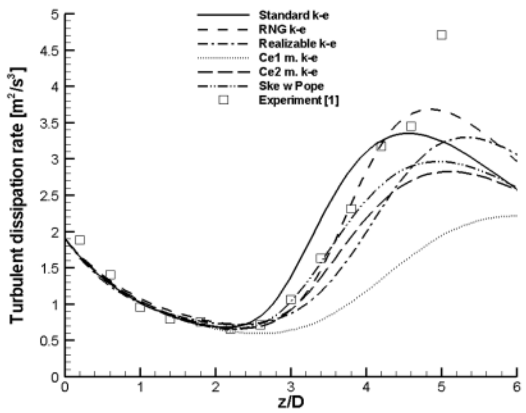

Figure 4. Turbulent dissipation rate distributions along normalized symmetry axis.

Turbulent kinetic energy profiles are also compared to the experiments (Figure 3). It is observed that all the variants of the k–ε model predict almost the same profiles up to onset of the turbulence core decay. After this point the results become different. They indicate that the homogeneous turbulence assumption used in experimental data processing is not applicable after the turbulence core decay.

Similar tendency is also observed in turbulent dissipation rate distribution in Figure 4. When turbulent core begins to decay the predictions of computations become different than measurements.

Reactive case studies are performed based on cold flow results. The premixed methane – air flow at 0.6 equivalence ratio is computed initially. In Figure 5, the results of Zimont and two CFM models are presented. The modeling results are also compared to the experiments.

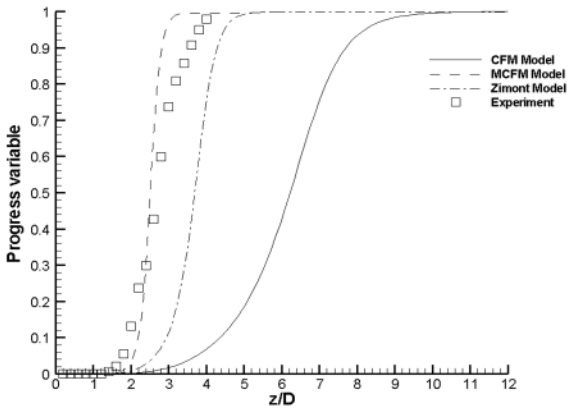

Figure 5. Comparison of the computed progress variable distribution to the experiments along axis.

It is observed that the model with original CFM model locates the flame front more downstream from the burner exit. In addition, it predicts wider progress variable profile, hence, thicker flame brush than experiments. Zimont model predicts similar progress variable profile with experiments. However, it locates the flame front slightly further downstream.

The modified CFM model shows the best agreement with the experiments. The flame front is computed near the middle region of the measured data. However, it predicts faster production rates of the products than experiments. Thus, the flame brush thickness is less.

The effect of the equivalence ratio is also investigated in present work. Simulations with three different equivalence ratios, namely 0.6, 0.7 and 0.8, are also performed with Zimont and MCFM models.

The comparison of the progress variable distribution along normalized axis for three different equivalence ratios, Figure 6, shows that further increase of the equivalence ratio results in steeper progress variable distribution. This effect of equivalence ratio on flame structure is also presented in [2, 9, 14]. Zimont model predicts more decrease in flame tip than in MCFM model with increase of the equivalence ratio. The profiles predicted by both models become relatively closer at higher equivalence ratio conditions.

The distributions of the reactant and product mass fractions predicted by the CFM model are presented in Figure 7. These distributions are obtained for one-step global methane–air reaction. The reactants are totally consumed within the reaction region which is at three-diameters after the burner exit.

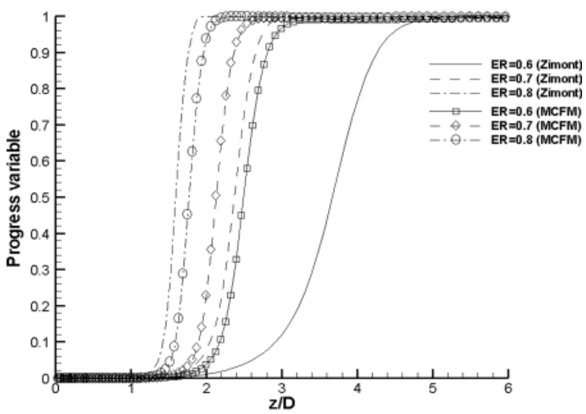

Figure 6. Comparison of the progress variable distribution, computed by Zimot model, along the axis for three different equivalence ratios (ER= Equivalence Ratio).

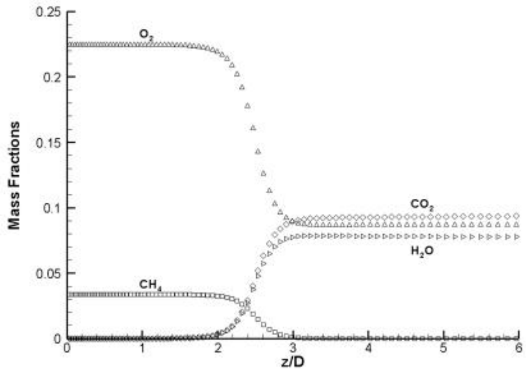

Figure 7. Species mass fraction distribution in normalized axial direction for ER=0.6.

5. Conclusion

The numerical simulations of the premixed turbulent combustion results obtained in ICARE are performed in this study. They are realized initially for the cold flow case in which air assumed to be the working fluid. The velocity and turbulent flow field are analyzed and compared to the experiments. Several variants of the k-ε turbulence model both provided by Fluent and modifications proposed for this model in several works are examined. The axial velocity profile in axial direction obtained by the k-ε model with $C_{\varepsilon 1}$ modification shows the best agreement with the experiments. The turbulent kinetic energy and dissipation rate profiles also agree with the experiments up to the turbulent core decay. The profiles become different after this position, which is at three-diameters downstream from the burner exit.

Reactive case studies are performed by means of different combustion models, namely Zimont and CFM models, for the premixed methane-air flow.

Premixed Zimont model is analyzed for 0.6, 0.7 and 0.8 equivalence ratio conditions. The model predicts the flame positions slightly further downstream comparing to experimental results. However, the progress variable profile is observed similar. The decrease in flame tip with increasing equivalence ratio is also observed in simulations.

The CFM model is also investigated. Besides the flame properties, species mass fractions are also examined. It is found that the CFM model locates the flame farther downstream from the burner exit. It predicts the progress variable distribution wider, that is, gives thicker flame brush. It is also observed that this model underestimates the flame surface density.

The modified version of the CFM model shows quantitatively and qualitatively good agreement comparing the experiments.

Acknowledgements

This work is supported within the international joint research project program between CNRS and TUBITAK (Project No. MAG-104M330). Baris YILMAZ is supported within the joint PhD grant by the French Embassy in Ankara as well as by the PhD support project (FEN-DKR-181005-0215) of BAPKO-Marmara University, Istanbul.

References

[1] T. Lachaux, Ph.D. Thesis, University of Orleans, France **(2004).**
[2] F. Halter, Ph.D. Thesis, University of Orleans, France **(2005).**
[3] G. Turpin, J. Troyes, AIAA-2000-3463, 36th AIAA/ASME/SAE/ASEE, Joint Propulsion Conference and Exhibit, Alabama USA**(2000).**
[4] R.C. Morgans, B.B. Dally, G.J. Nathan, P.V. Lanspeary, D.F. Fletcher, 2nd International Conference on CFD in the Minerals and Process Industries 1999 Australia**(1999).**
[5] S.B. Pope, AIAA Journal, 16/3 **(1978)** 279-281.
[6] D. Davidenko, I. Gökalp, E. Dufour, P. Magre, 13th AIAA/CIRA International Space Planes and Hypersonic Systems and Technologies Conference, Italy **(2005).**
[7] V. Zimont, W. Polifke, M. Bettelini, W. Weisenstein, J. of Gas Turbines Power, 120 **(1998)** 526-532.
[8] V. Zimont. Exp. Thermal and Fluid Science, 21 **(2000)** 179-186.
[9] S. P. R. Muppala, N. K. Aluri, F. Dinelacker, A. Leipertz, Combustion and Flame 140 **(2005)** 257-266.
[10] T. Poinsot, D. Veynante, Theoretical and Numerical Combustion, R.T. Edwards Publications **(2001)**.
[11] J.M. Duclos, D. Veynante, T. Poinsot, Combustion and Flame 95 **(1993)** 101-117.

[12] R. O. S. Prasad, J. P. Gore, Combustion and Flame 116 **(1999)** 1-14.
[13] N. K. Aluri, Q. Sha, S. P. R. Muppala, F. Dinelacker, Proc. of the ECM **(2005)** 132.
[14] C. Cohé, F. Halter, C. Chauveau, I. Gökalp, Ö. Gülder, Proc. Combust. Inst. 31 **(2007)** 1345 – 1352.
[15] Fluent 6.2 Users Manual.
[16] CHEMKIN II Users Manual